

# Measurements of corner cubes microstructures by high-magnification digital holographic microscopy

Jonas Kühn\*<sup>a</sup>, Etienne Cuche<sup>b</sup>, Yves Emery<sup>b</sup>, Tristan Colomb<sup>a</sup>, Florian Charrière<sup>a</sup>,  
Frédéric Montfort<sup>b</sup>, Mikhail Botkine<sup>b</sup>, Nicolas Aspert<sup>b</sup> and Christian Depeursinge<sup>a</sup>

<sup>a</sup>Ecole Polytechnique Fédérale de Lausanne (EPFL), Institute of Imaging and Applied Optics,  
CH-1015 Lausanne, SWITZERLAND;

<sup>b</sup>Lyncée Tec SA, PSE-A, CH-1015 Lausanne, SWITZERLAND

## ABSTRACT

This paper presents Digital Holographic Microscopy (DHM) quantitative measurements of transparent high aspect-ratio microstructures. Our experiment was performed using a digital holographic microscope in transmission configuration with a 60x magnification 1.3 NA oil immersion microscope objective, with a diode laser source at 664 nm. We used a calculation model based on the use of two immersion liquids for the experiment, the first one to resolve the phase jumps by using a refractive index liquid close to the sample index, in combination with a second one to retrieve the sample topology from the optical path length information. Such a model makes absolute topographic measurements of high aspect ratio transparent samples achievable by DHM. The model is then applied to measure 25 and 50  $\mu\text{m}$  transparent micro-corner cubes arrays, which exhibit up to 1:1,4 aspect ratio with theoretical slopes up to about 55 degrees. Thanks to our phase measurement precision down to  $1^\circ$ , we found possible to measure accurately the slopes of each face of the microstructures under investigation, and this with a good theoretical agreement.

Keywords: Microscopy, digital holography, high aspect-ratio, transparent microstructures, corner cube, metrology

## 1. INTRODUCTION

Digital holographic microscopy is a technique which enables digital reconstruction of holograms acquired by a Charge Coupled Device (CCD) camera with a computer. In a similar way like in classical holography [1], and thanks to the progress in computer performances during the past decades, the diffraction of a wavefront by the hologram can be computed [2, 3] and numerically propagated along a reconstruction distance to any chosen observation plane. The numerical knowledge of the complex wavefront allows computation of the amplitude [4] and noticeably the phase [5, 6, 7], which leads to nanometer-scale quantitative measurements along the optical axis (lateral resolution is diffraction-limited). This gives access to the optical path length, refractive index or shape of the specimen under investigation, either in transmission or in reflection configuration. Moreover, the use of CCD cameras enables high-speed real-time measurements, and wavefront deformations (aberrations, or even specimen shape) are easily corrected or compensated digitally [8]. Nowadays, DHM finds numerous applications ranging from real-time Micro Electro Mechanical Systems (MEMS) monitoring [9], micro-optics components inspection [10], micro-components topology measurements, surface roughness characterization to biological samples observations [11, 12, 13], or even analysis of the birefringence properties [14].

In this study, we apply DHM to quantitatively characterize high aspect-ratio microstructures with a 60x magnification Microscope Objective (MO) in a transmission configuration setup. Digital holographic measurements are performed on a transparent UV copy of micro-corner cube arrays metal shim, provided by the Fraunhofer-Institut für Siliziumtechnologie (ISIT). The fabrication process involved is graytone lithography as described in Refs. 15, 16 and 17. High aspect ratio periodic microstructures can be used to design various optical micro-devices such as Fresnel lenses, segmented mirrors, or retro reflectors [18, 19]. These last ones are indeed usually based on a corner cube geometry and their application range goes from traffic light backreflectors to the security printing industry kinegrams, integrated in modern ID cards or banknotes.

\*jonas.kuehn@a3.epfl.ch, phone +41216933742, fax +41216933701; <http://apl.epfl.ch/page12232.html>

Until now, typical technologies for imaging this kind of structures relied on Scanning Electron Microscopy (SEM) [20, 21] or Scanning Probe Microscopy (SPM) [22], but they are either difficult to convert in quantitative datas or based on a surface-contact, point-by-point scanning approach.

It will be shown that DHM makes it possible to gather in one technique both the contactless full-field-of-view and quantitative measurements approaches. To illustrate this capability, the technique will be applied to retrieve precise numerical slopes datas for down to 25  $\mu\text{m}$  lateral size micro corner cubes, with up to 1:1,4 aspect ratio over a 110  $\mu\text{m}$  field of view, with a two-steps procedure based on a change of the immersion medium.

## 2. METHODOLOGY

### 2.1 Acquisition and reconstruction of the digital hologram

The configuration used in this experiment is a transmission DHM, which mainly consists in a Mach-Zehnder interferometer setup combined with a MO and a CCD camera, as presented below in Fig.1.

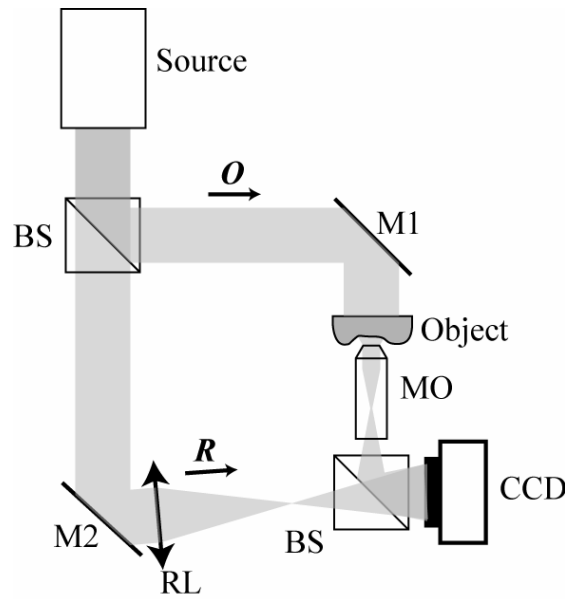


Figure 1: Experimental Configuration. O, object wave; R, reference wave; BS, beam-splitter; M1, M2 mirrors; RL, reference lens, which matches the curvature induced on the object wave by the microscope objective (MO)

The laser beam emitted by the source, here a 664nm laser diode, is splitted into two parts: the reference beam (R) and the object beam (O). After having interacted with the sample, the object beam is collected by the MO (here a 60x, 1.3NA oil immersion MO), recombined with the reference wave, and the interference is recorded on a CCD camera. The image plane of the MO is located approximately 5 cm behind the camera, and the holographic configuration can be considered as if the object were replaced by the magnified image of the object by the MO [7].

The resulting hologram intensity  $I_H$  recorded on the CCD can be written as:

$$I_H(x, y) = |R|^2 + |O|^2 + RO^* + R^*O \quad (1)$$

Considering the off-axis configuration, it is feasible to select only the virtual image complex term  $R^*O$  of Equ. 1 in the Fourier domain of the hologram plane, according to Cuche *et al.* in [23]. This complex wavefront can therefore be propagated to any plane of reconstruction according to the Fresnel approximation:

$$\Psi(\xi, \eta) = \Phi(\xi, \eta) \cdot \frac{\exp(i2\pi d/\lambda)}{i\lambda d} \cdot \exp\left[\frac{i\pi}{\lambda d}(\xi^2 + \eta^2)\right] \cdot \iint R_D(x, y) I_H(x, y) \exp\left[\frac{i\pi}{\lambda d}((x - \xi)^2 + (y - \eta)^2)\right] dx dy \quad (2)$$

In the expression above,  $\Psi$  is the reconstructed wavefront in the coordinate  $O\xi\eta$  at a distance  $d$  from the hologram plane  $Oxy$ ,  $\lambda$  is the wavelength,  $R_D$  is a digital replica of the reference wave  $R$  (Equ. 1) and  $\Phi$  is a phase mask designed to compensate for the curvature induced by the MO and the remaining aberrations. The discrete counterpart of Equ. 2 can be implemented for computation as follow:

$$\Psi(m, n) = \Gamma(m, n) \cdot \frac{\exp(i2\pi d/\lambda)}{i\lambda d} \cdot \text{FFT} \left\{ R_D(k, l) I_H(k, l) \exp\left[\frac{i\pi}{\lambda d}(k^2 \Delta x^2 + l^2 \Delta y^2)\right] \right\}_{m, n} \quad (3)$$

Where FFT is the Fast Fourier Transform operator,  $\Gamma$  is a modified digital phase mask which fuses  $\Phi$  and the quadratic term outside the integral in Equ. 2,  $k, l, m$  and  $n$  are integers ( $-N/2 \leq k, l, m, n < N/2$ ),  $N$  the number of pixel of the CCD camera,  $\Delta x$  and  $\Delta y$  are the pixel size and  $R_D$  is defined as:

$$R_D(k, l) = \exp[i(k_x k \Delta x + k_y l \Delta y)] \quad (4)$$

with  $k_x$  and  $k_y$  the tilt parameters that should be adjusted to match the reference wave  $R$  used for the hologram recording.

Both the digital reference wave  $R_D$  parameters and the digital phase mask  $\Gamma$  can easily be adjusted in real-time with a polynomial fit procedure as described by Colomb *et al.* in [8], which permits a single-hologram reconstruction.

This access to the quantitative complex wavefront enables to extract both information about the amplitude, similar to classical microscopy, and noticeably the phase for wavelength-range nanometric measurements along the optical axis, as presented in Fig. 2. Minimum deviation of the phase value over the Field Of View (FOV) is down to about  $1^\circ$ , and means nanometric resolution in the case of a topographic reflection experiment. Regarding transmission measurements, the phase information is directly related to the integrated Optical Path Length (OPL) along the optical axis through the sample. Lateral resolution remains diffraction-limited, though.

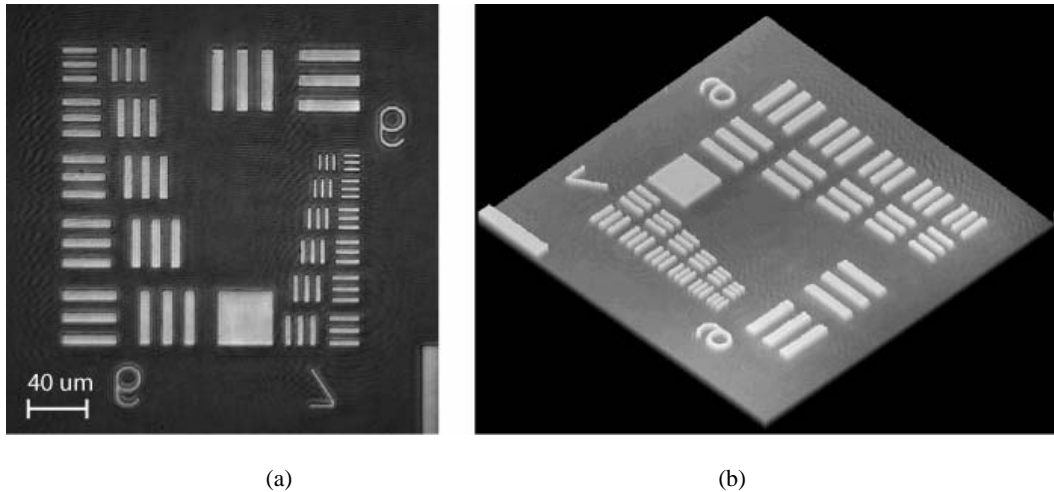


Figure 2. USAF test target (50 nm thickness chromium deposit on glass) in 20x magnification reflection DHM  
(a) Amplitude-contrast image, (b) Quantitative phase image in 3D perspective view

## 2.2 Transparent microstructures measurements by digital holography microscopy

### 2.2.1 Resolving the phase jumps of high aspect-ratio structures

The ability to measure high aspect-ratio samples is conditioned by the assumption that the phase jumps induced by the OPL through the object are resolved laterally and fully sampled by the CCD camera pixels. A critical parameter is the lateral resolution of the configuration, diffraction-limited by the NA of the MO: one phase jump should not occur between two points with a lateral separation smaller than the Airy disc radius, otherwise it won't be resolved by the MO, and furthermore not recorded on the camera. In this experiment, the use of a high-NA MO is precisely intended to fulfill this requirement.

As the range of aspect-ratio values accessible with this MO is still too limited for the microstructures involved here, there is also a strong need to reduce the number of phase jumps by using an immersion medium, as illustrated in Fig. 3:

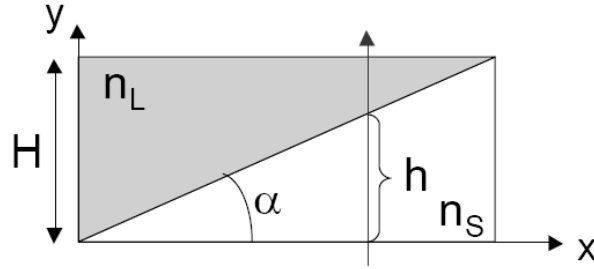


Figure 3. Measurement of the slope of an object in an immersion liquid.  $H$ , total height;  $n_s$  refractive index of the sample;  $n_L$  refractive index of the immersion liquid;  $\alpha$  angle of the slope to measure

Let us consider the phase corresponding to the OPL of a beam travelling through the transparent sample along the arrow in Fig. 3:

$$\phi(x) = \frac{2\pi}{\lambda} OPL(x) = \frac{2\pi}{\lambda} \{n_s h(x) + n_L [H - h(x)]\} = \frac{2\pi}{\lambda} [(n_s - n_L)h(x) + n_L H] \quad (5)$$

For the same physical dimensions, the measured phase difference slope  $p$  will be reduced compared with an experiment in air ( $n_L=1$ ) :

$$p = \frac{d\phi(x)}{dx} = \frac{2\pi}{\lambda} (n_s - n_L) \frac{dh(x)}{dx} \quad (6)$$

This is a simple way to drastically reduce the frequency of phase jumps for high aspect ratio structures, allowing them to be observed by DHM or other interferometric technique. The singular case is a matching refractive index between the sample and the immersion medium ( $n_L = n_s$ ), where the micro-structures becomes "invisible" from the phase point of view.

### 2.2.2 Method to extract the slope angle of the microstructures

Assuming a constant slope, and writing  $h(x) = \tan(\alpha) x$  from Fig. 3, the slope angle  $\alpha$  can be derived from Equ. 6:

$$\alpha = \arctan \left[ \frac{p\lambda}{2\pi(n_s - n_L)} \right] \quad (7)$$

However, the hypothesis of an a-priori knowledge of the sample refractive index  $n_s$  is usually not fulfilled. Therefore, an additional calibrated immersion liquid is needed. If the experiment is conducted twice with two different immersion liquids with refractive indexes  $n_{L1}$  and  $n_{L2}$ , the following profiles can be extracted:

$$\begin{cases} p_1 = \frac{2\pi}{\lambda}(n_s - n_{L1}) \tan \alpha \\ p_2 = \frac{2\pi}{\lambda}(n_s - n_{L2}) \tan \alpha \end{cases} \quad (8)$$

The sample refractive index is now available from Equ. 8:

$$n_s = \frac{p_1 n_{L2} - p_2 n_{L1}}{p_1 - p_2} \quad (9)$$

And finally the calculus of the slope angle with this two-steps procedure is given by:

$$\alpha = \arctan \left[ \frac{(p_2 - p_1)\lambda}{2\pi(n_{L1} - n_{L2})} \right] \quad (10)$$

which is, as expected, independent from the refractive index of the object.

In summary, by performing two successive experiments with the use of two well-calibrated immersion liquids, it's possible to simultaneously resolve the phase jumps of high aspect-ratio microstructures and extract the numerical slope angle - without knowledge of the transparent sample refractive index.

### 3. MEASUREMENTS

#### 3.1 Experimental considerations

The samples investigated here are transparent UV copies of the metal schim of micro-corner cubes arrays of 50  $\mu\text{m}$  and 25  $\mu\text{m}$  base dimension. Used as retro reflectors, these kinds of structures should present an aspect-ratio of more than 1:1,4, as the slope angles of the tetrahedron faces are expected to reach the 54,74° value, given by simple geometry considerations. A Scanning Electron Microscope (SEM) picture of this kind of periodic structures is presented in Fig. 4:

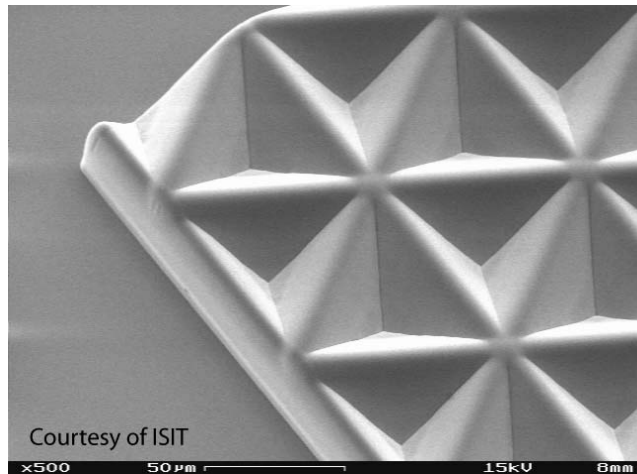


Figure 4. SEM image of the 50  $\mu\text{m}$  micro-corner cubes array investigated

The maximum FOV provided by the 60x 1.3NA MO is about 110  $\mu\text{m}$  with a 1024x1024 6.45  $\mu\text{m}$  pixels CCD camera for the hologram acquisition. For the two-steps procedure described in Section §2.2.2, we have used a certified immersion liquid solution as immersion medium #1 ( $n_{L1} = 1.405 @ 656.3\text{nm}$ ) and distilled water as immersion medium #2 ( $n_{L2} = 1.332 @ 664\text{nm}$ ). Typical standard deviation over a small area inside the FOV is about 1° in phase, and the

lateral resolution expected with this high-aperture MO is about 300 nm, having pointed out the satisfied Nyquist condition regarding the CCD sampling (pixel size of 6.45  $\mu\text{m}$  for a 60x magnification). A hologram of this retro reflectors array is presented below in Fig. 5, along with the reconstruction in amplitude and phase for three different positions of the sample along the optical z-axis (the object is physically displaced):

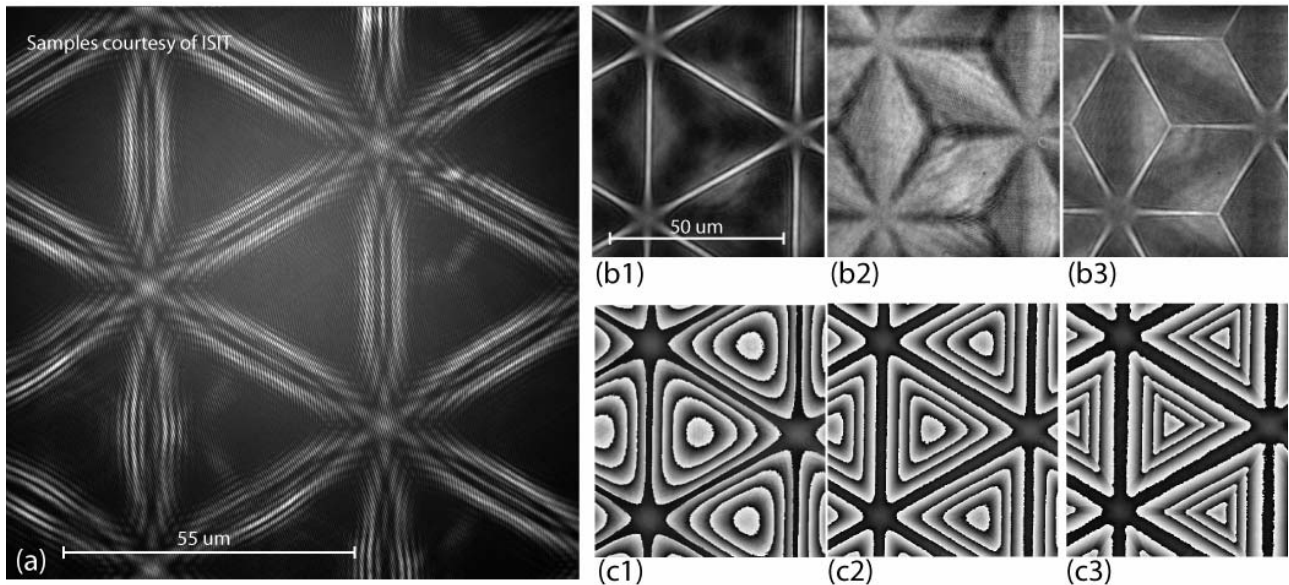


Figure 5. DHM images of the sample. (a) Hologram, (b) Intensity images, (c) Phase-contrast images, (1) Focus on top, (2) Intermediate focus (5  $\mu\text{m}$  below), (3) Focus on the bottom (10  $\mu\text{m}$  below)

The positive effect of the immersion solution is clearly seen above in Fig. 5c, where the phase jumps induced by the corner cubes structures are well-defined and easily sampled. Due to the use of a high-magnification MO, and because of the high aspect-ratio of this kind of retro reflectors structure, the limitation of the depth of field is to be considered. As shown in Fig. 5, it's not possible to have an accurate focus on both the corner cube upper edge and bottom region because the structure height exceed the depth of field of the MO, around 300nm in this case. For this reason, all the following measurements are taken in the intermediate focus position and, as presented in Fig. 6, the error on the slope calculus is negligible if only the central slope pixels are taken into account:

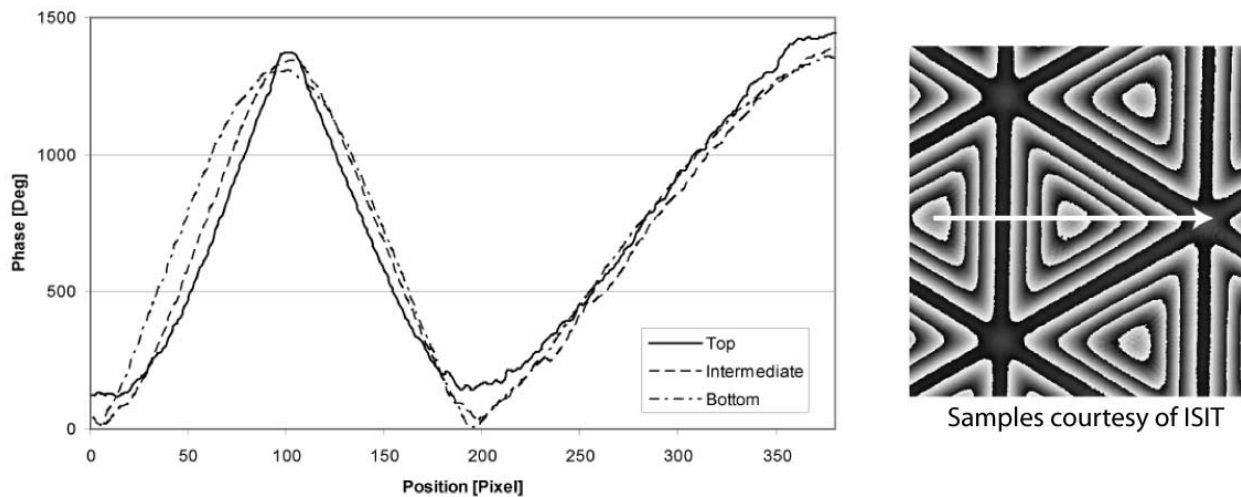


Figure 6. Slope profiles along the white arrow for the three focus position: slopes values remain comparable despite defocus. (1 pixel = 230 nm lateral)

### 3.2 Results

Typical DHM images of this transparent micro corner cubes array are exposed in Fig. 7, with the use of the immersion medium #1 at the intermediate focus position, as explained above in Section §3.1:

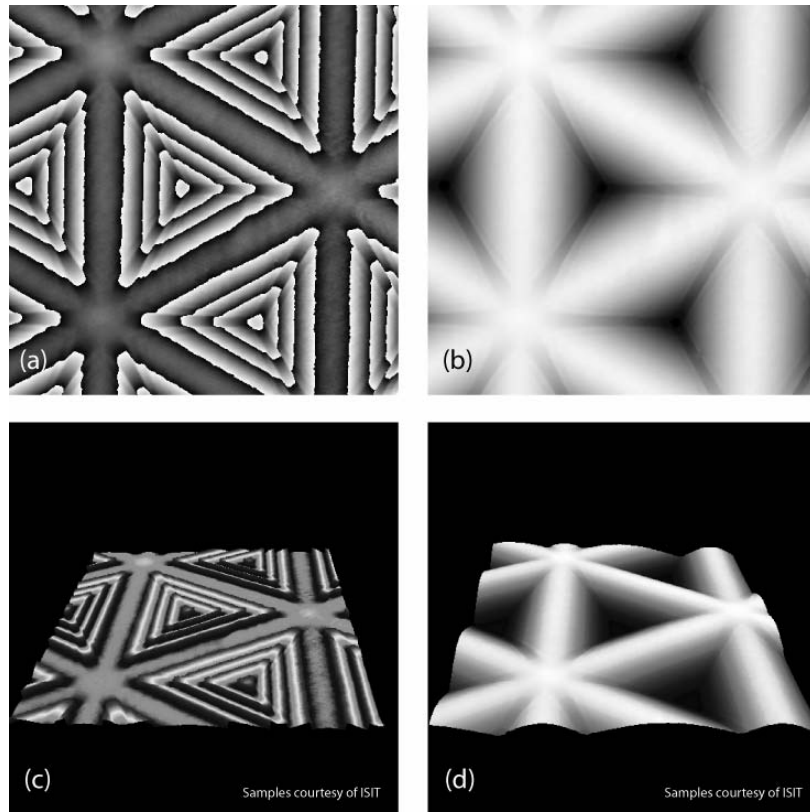


Figure 7. Micro corner cubes imaging by DHM. (a) Raw phase-contrast image, (b) Unwrapped phase, (c) 3D view of (a), (d) 3D view of (b)

Thanks to the quantitative information contained in the phase datas, it's now possible to measure the slopes in both immersion liquids, following the procedure explained in section §2.2.2. Fig. 8 demonstrates the calculus of the sample refractive index based on the two-steps approach:

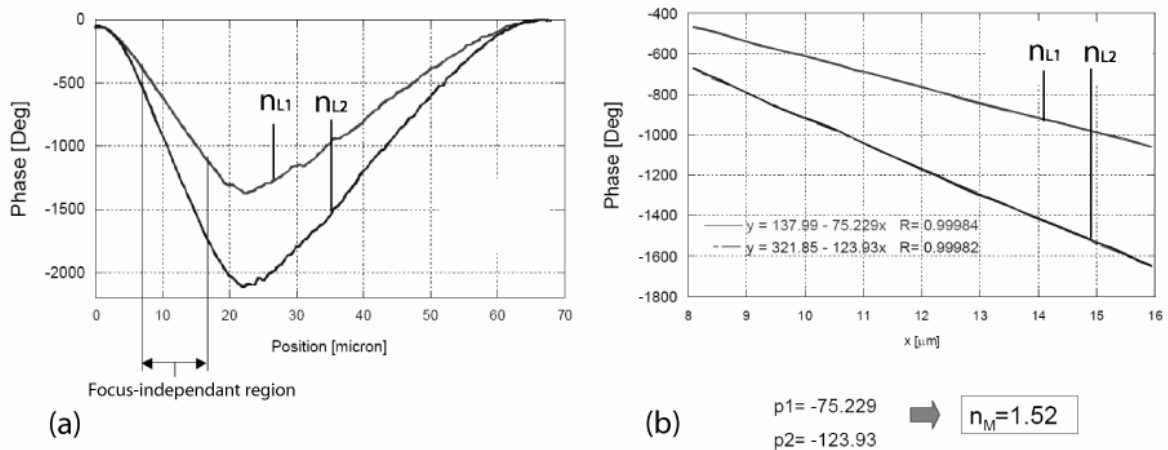


Figure 8. Two-steps calculation of the sample refractive index. (a) Slopes extraction, (b) Sample refractive index calculation

Given the precision on the refractive indexes of the two immersion liquids used in the experiment (checked with a refractometer), and the 1° only phase deviation, the slopes estimation can be considered as very accurate. Even if an imprecision of the lateral scale determination is possible, considering the limited precision of the FOV, this should not affect the results as stated by Equ. 9. However for practical reasons, measurements with the two different immersion mediums were not performed precisely on the same structure area. In case of angles variations between micro corner cubes, this prevents a rigorous estimation of our precision for the sample refractive index measurement.

Thanks to the expression in Equ. 10, the quantitative calculus of the slopes angles is now possible. Results for the 50 μm micro corner cubes array are presented in Fig. 9:

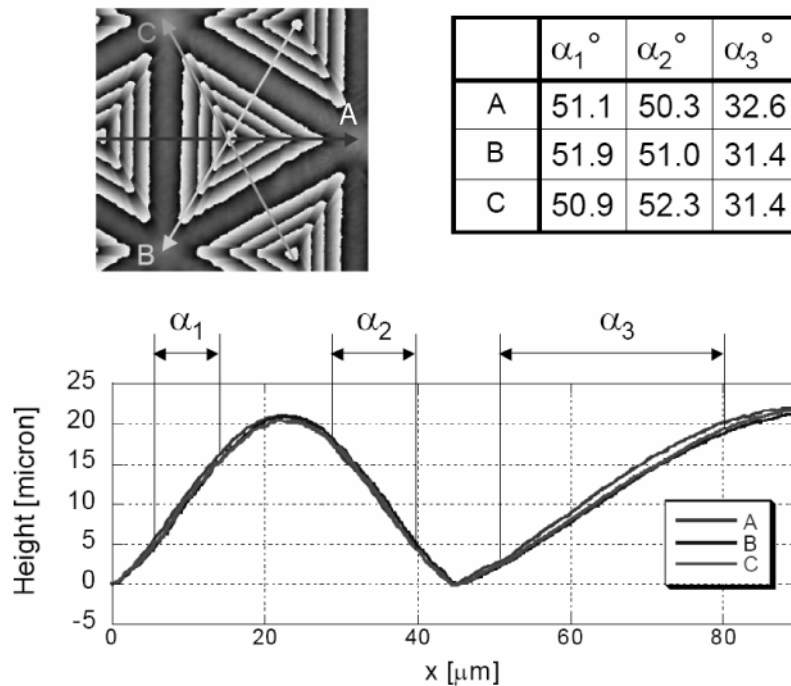


Figure 9. Determination of the slope angles  $\alpha_i$  for the three faces of a 50 μm micro corner cube

The face angles  $\alpha_1$  and  $\alpha_2$  should be equals to 54,74° in Fig. 9, to respect the corner cube geometry, which is critical regarding the retro reflection this kind of structures are designed for. In a similar way,  $\alpha_3$  values should match the angle of 35,26° to guarantee the top angle value of 90°. But in our case we are systematically too low for both angles, and the sum angle does not exceed 82-84° instead of 90°, indication of a faulty device. In top of that,  $\alpha_1$  and  $\alpha_2$  numerical values should be comparables but here the difference can exceed 1,5° in certain cases. This matches the feedback provided by the sample provider ISIT, who confirmed these micro corner cubes arrays were not selected as they did not pass the quality test.

To validate the DHM ability to measure smaller structures, similar results with 25  $\mu\text{m}$  base corner cube array are shown below in Fig. 10. In this case, the faces angles are even smaller than with the 50  $\mu\text{m}$  corner cubes, in respect to the expected 54,74° and 35,26° values.

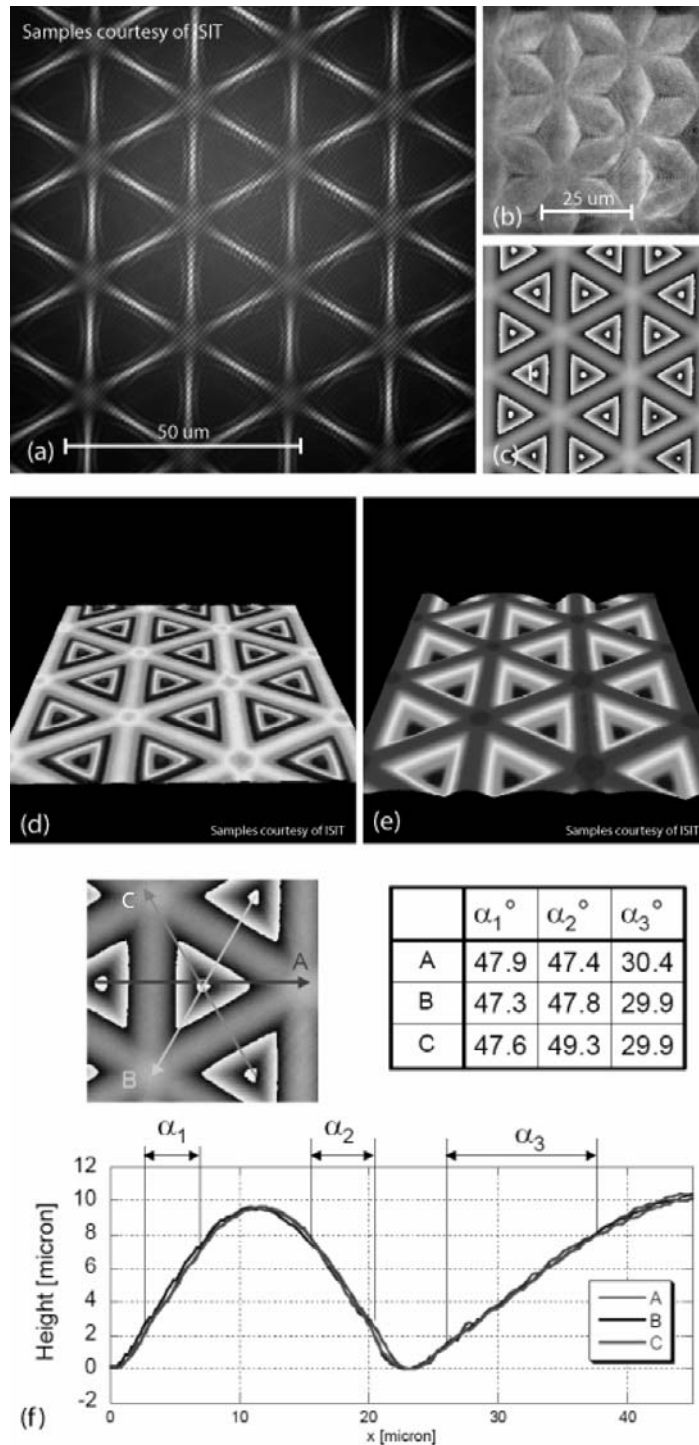


Figure 10. DHM measurements of 25  $\mu\text{m}$  transparent corner cubes array. (a) Hologram, (b) Amplitude image, (c) Phase image, (d) 3D view of the wrapped phase, (e) Unwrapped phase 3D view, (f) Extraction of the corner cubes faces angles

## 4. CONCLUSIONS

In this paper, we demonstrated the effectiveness of digital holographic microscopy (DHM) for industrial characterization of high aspect-ratio microstructures, with a nanometer resolution along the optical axis, and the compatibility of the method with high magnification up to 1.3NA microscope objective. We have shown that DHM in transmission is an appropriate tool for quantitative measurements of transparent microstructures. The ability to resolve high aspect-ratio samples can be guaranteed with the use of an immersion liquid with a refractive index close to the object index. In such a case, the limited depth of field of the MO remains a limitation, though. Moreover, a two-immersion mediums approach has been presented, which enables a contactless, full-field-of-view and precise measurements of both the object refractive index and micro-structures angles, independently from the lateral calibration. Finally, quantitative numerical results for both 25 and 50  $\mu\text{m}$  base dimension micro-corner cubes were obtained, and appear to be on good agreement with the qualitative feedback of the samples provider.

## 5. ACKNOWLEDGEMENTS

The authors would like to thank Dr. Klaus Reimer from the Fraunhofer-Institut für Siliziumtechnologie (ISIT) for providing the samples and for the fruitful feedbacks. The development of the technology has been supported by Swiss government through CTI grants TopNano 21 #6101.3 and NanoMicro #6606.2 and #7152.1. Systems are commercialized by Lyncée Tec SA (<http://www.lynceetec.com/>).

## REFERENCES

1. D. Gabor, "A new microscopic principle", *Nature*, 1948
2. J. W. Goodman and R. W. Lawrence, "Digital image formation from electronically detected holograms," *Appl. Phys. Lett.* 11, 77–79 (1967).
3. T. Huang, "Digital holography", *Proc. IEEE*, 59, no. 9, 1971, 1292-1304
4. U. Schnars and W. Jüptner. "Direct recording of holograms by a CCD target and numerical reconstruction" *Appl. Opt.* 33(2): 179–181 (1994)
5. U. Schnars. "Direct phase determination in hologram interferometry with use of digitally recorded holograms" *J. Opt. Soc. Am. A* 11: 2011–2015 (1994)
6. E. Cucho, F. Bevilacqua and C. Depeursinge. "Digital holography for quantitative phase-contrast imaging" *Opt. Lett.* 24(5): 291–293 (1999)
7. E. Cucho, P. Marquet and C. Depeursinge. "Simultaneous amplitude-contrast and quantitative phase-contrast microscopy by numerical reconstruction of Fresnel off-axis holograms". *Appl. Opt.* 38(34): 6994–7001 (1999)
8. T. Colomb, E. Cucho, F. Charrière, J. Kühn, N. Aspert, F. Montfort, P. Marquet, and C. Depeursinge. "Automatic procedure for aberrations compensation in digital holographic microscopy and applications to specimen shape compensation". *Appl. Opt.* 45(5): 851–863 (2006)
9. G. Coppola, P. Ferraro, M. Iodice, S. D. Nicola, A. Finizio and S. Grilli. "A digital holographic microscope for complete characterization of microelectromechanical systems". *Measurement Science and Technology* 15(3): 529–539 (2004)
10. F. Charrière, J. Kühn, T. Colomb, F. Montfort, E. Cucho, Y. Emery, K. Weible, P. Marquet, and C. Depeursinge. "Characterization of microlenses by digital holographic microscopy". *Appl. Opt.* 45(5): 829–835 (2006)
11. D. Carl, B. Kemper, G. Wernicke and G. von Bally. "Parameter-optimized digital holographic microscope for high-resolution living-cell analysis". *Appl. Opt.* 43(36): 6536–6544 (2004)
12. P. Marquet, B. Rappaz, P. J. Magistretti, E. Cucho, Y. Emery, T. Colomb and C. Depeursinge. "Digital holographic microscopy: a noninvasive contrast imaging technique allowing quantitative visualization of living cells with subwavelength axial accuracy". *Opt. Lett.* 30(5): 468–470 (2005)
13. B. Rappaz, P. Marquet, E. Cucho, Y. Emery, C. Depeursinge and P. J. Magistretti. "Measurement of the integral refractive index and dynamic cell morphometry of living cells with digital holographic microscopy". *Opt. Express* 13(23): 9361 – 9373 (2005)

14. T. Colomb, F. Dürr, E. CuChe, P. Marquet, H. G. Limberger, R.-P. Salathé, and C. Depeursinge. "Polarization microscopy by use of digital holography: application to optical-fiber birefringence measurements". *Appl. Opt.* 44(21): 4461–4469 (2005)
15. Döldissen, H. Engel, J. Wengelink and H.J. Hensel, „Lithographic fabrication of integrated micro-optical elements“, *Proc. Eur. Conf. Int. Optics (ECIO '93)*, Neuchatel, Switzerland, pp. 4-10, April 1993
16. R. Purdy, „Fabrication of complex micro-optic components using photo-sculpting through half-tone transmission masks“, *IOP Conf., Focus on Micromechanics*, Warwick, IOP Publishing, London, June 1993
17. K. Reimer, R. Engelke, U. Hofmann, P. Merz, K.T. Kohlmann v. Platen, B. Wagner. „Progress in Graytone Lithography and Replication Techniques for Different Materials“. *Proc. of Micromachine Technology for Diffractive and Holographic Optics*, Santa-Clara 1999, SPIE Vol. 3879, p. 98
18. K. Reimer, H.J. Quenzer, M. Jürs, B. Wagner, „Micro-optic fabrication using one-level gray tone lithography“, *Proc. Of Photonics West*, San Jose 1997, SPIE Vol. 3008, p. 279
19. K. Reimer, U. Hofmann, M. Jürs, W. Pilz, H.J. Quenzer, B. Wagner, „Fabrication of Microrelief Surfaces using a onestep lithography process“, *Proc. Of Micromachining and Microfabrication*, Austin 1997, SPIE Vol. 3226, p. 2
20. P. W. Trimby, D. J. Prior, "Microstructural imaging techniques: a comparison between light and scanning electron microscopy", *Tectonophysics* 303: 71-81 (1999)
21. B. Minnich, H. Leeb, E. W. N. Bernroider, A. Lametschwandtner, "Three-dimensional morphometry in scanning electron microscopy: a technique for accurate dimensional and angular measurements of microstructures using stereopaired digitized images and digital image analysis", *Journal of Microscopy* 195(1): 23-33 (1999)
22. B. A. Sexton, R. J. Marnock, "Characterization of High Resolution Resists and Metal Shims by Scanning Probe Microscopy", *Microsc. Microanal.* 6: 129-136 (2000)
23. E. CuChe, P. Marquet, and C. Depeursinge, "Spatial filtering for zero-order and twin-image elimination in digital off-axis holography," *Appl. Opt.* 39 (23), 4070-4075 (2000).